*Exploration Geophysics (2004) **35**, 251–254*

Using Mohr circles to identify regional dimensionality and strike angle from distorted magnetotelluric data

John T. Weaver[1] **F.E.M. (Ted) Lilley**[2]

Key Words: Mohr circles, magnetotellurics, impedance tensor, phase tensor, invariants

ABSTRACT

Mohr circles have recently been used as an aid in the analysis of the magnetotelluric (MT) impedance tensor. Although well known as a representation of the stress tensor in elasticity theory, the potential application of Mohr circles to MT data was virtually unrecognised by the geoelectromagnetic induction community until the pioneer paper of Lilley (1976). An important difference between the stress tensor and the MT tensor is that the former is real while the latter is complex, which means that the MT tensor must be represented by two Mohr circles rather than one. Although early discussions on the behaviour of MT data concentrated mainly on the real part of the MT tensor, it became necessary in more detailed treatments to consider both real and imaginary Mohr circles together. In particular, identification of seven independent invariants of the complex MT tensor as geometric invariants on a Mohr circle diagram, and their physical interpretation, required the two Mohr circles to be plotted together. A significant advance has been made with the introduction of the (real) phase tensor by Caldwell, Bibby, and Brown (2004). Although the phase tensor has only three independent invariants, it has been shown by Weaver, Agarwal, and Lilley (2003) that they retain the important physical properties of the seven invariants of the MT tensor introduced earlier but with the distinct advantage that they can be displayed graphically in a single Mohr circle diagram. In particular, identification of the dimensionality of the regional conductivity structure becomes a straightforward matter whether or not the data are distorted by near-surface conductivity anomalies.

INTRODUCTION

Under a right-handed rotation of the x and y axes in a rectangular coordinate system (x, y, z), through an angle θ about the positive z-axis, any 2×2 real matrix

$$\mathbf{T} = \begin{pmatrix} T_{11} & T_{12} \\ T_{21} & T_{22} \end{pmatrix} \equiv \begin{pmatrix} \tau_1 + \tau_3 & \tau_2 + \tau_4 \\ \tau_2 - \tau_4 & \tau_1 - \tau_3 \end{pmatrix}, \qquad (1)$$

where $\tau_1 = (T_{11} + T_{22})/2$, $\tau_2 = (T_{12} + T_{21})/2$, $\tau_3 = (T_{11} - T_{22})/2$, and $\tau_4 = (T_{12} - T_{21})/2$, takes the form

$$\mathbf{T}' = \begin{pmatrix} \tau_1 + \tau_0 \cos 2(\theta_\tau - \theta) & \tau_0 \sin 2(\theta_\tau - \theta) + \tau_4 \\ \tau_0 \sin 2(\theta_\tau - \theta) - \tau_4 & \tau_1 - \tau_0 \cos 2(\theta_\tau - \theta) \end{pmatrix} \qquad (2)$$

in the rotated coordinate system (x', y'). Here we have defined $\tau_0 = (\tau_2^2 + \tau_3^2)^{1/2}$ and $\tan 2\theta_\tau = \tau_2/\tau_3$. It follows at once from equation (2) that

$$(T'_{11} - \tau_1)^2 + (T'_{12} - \tau_4)^2 = \tau_0^2 , \qquad (3)$$

which represents a circle, centre (τ_1, τ_4), radius τ_0, in the plane of T'_{11} and T'_{12}. This is an example of the Mohr circle first used to depict graphically the real, symmetric stress tensor in continuum mechanics. (Symmetry implies $\tau_4 = 0$, but as we see from the derivation above, this is by no means a necessary condition for the Mohr circle representation to be valid.) Note that the three well-known rotational invariants of a second-rank tensor $\mathbf{T}$, namely its trace, determinant, and the difference dif $\mathbf{T}$ of its off-diagonal terms, are closely related to the radius of the circle and the coordinates of its centre, i.e., tr $\mathbf{T} = 2\tau_1$, dif $\mathbf{T} = 2\tau_4$ and $(\text{tr}\,\mathbf{T})^2 + (\text{dif}\,\mathbf{T})^2 - 4\det\mathbf{T} = 4\tau_0^2$.

An alternative expression to (1) for the tensor in its given frame of reference is obtained by setting $\theta = 0$ in (2):

$$\mathbf{T} = \begin{pmatrix} \tau_1 + \tau_0 \cos 2\theta_\tau & \tau_0 \sin 2\theta_\tau + \tau_4 \\ \tau_0 \sin 2\theta_\tau - \tau_4 & \tau_1 - \tau_0 \cos 2\theta_\tau \end{pmatrix} . \qquad (4)$$

In this form, the tensor is clearly defined in terms of its three independent rotational invariants, τ_1, τ_4, and τ_0, and an angle θ_τ that defines the orientation of the axes in which the given tensor components are measured. It can be seen from (2) that θ_τ is the angle through which the axes of measurement must be rotated in order for the diagonal elements to attain their maximum or minimum values.

In magnetotelluric (MT) studies, data are usually supplied as the complex-valued components of the MT tensor $\mathbf{M}$, defined by $\mathbf{e} = \mathbf{M}\mathbf{b}$ where $\mathbf{e} = (e_1, e_2)^T$ and $\mathbf{b} = (b_1, b_2)^T$ are (complex) column vectors representing the spatial parts of the horizontal x and y components of the electric and magnetic fields on the earth's surface $z = 0$ (z positive downwards into the earth). Their time-dependence is expressed by a factor $\exp(i\omega t)$, which cancels out in the defining equation above. Unlike the stress tensor, the MT tensor is neither real nor symmetric. Lilley (1976) recognised, however, that the locus of its *real* part as the horizontal axes rotated could be displayed graphically as a Mohr circle in the $(\text{Re}M'_{11})(\text{Re}M'_{12})$-plane, which was an interesting alternative to other graphical depictions in use at the time.

Almost two decades elapsed before Lilley (1993a, b, c) actually used Mohr circles as a visual aid in the analysis of real data. He treated the real and imaginary parts of the MT tensor separately, each with its own Mohr circle representation. Earlier, Eggers

[1] *Department of Physics & Astronomy*
University of Victoria
Victoria, BC
Canada V8W 3P6
Email: weaver@phys.uvic.ca

[2] *Research School of Earth Sciences*
Australian National University
Canberra, ACT 0200
Australia
Email: Ted.Lilley@anu.edu.au

Presented at the 17th ASEG Geophysical Conference & Exhibition, August 2004.
Revised manuscript received: November 7, 2004.

(1982) had taken the complex nature of the MT tensor into account by displaying the loci of its components M'_{ij} (i = 1,2; j = 1,2) under a rotation of the axes, as ellipses traced out in the *complex* (Re M'_{ij})(Im M'_{ij})-plane. Although all essential information about the MT tensor was contained in the geometric properties of such ellipses, Mohr circles offered advantages in their visual appeal. They permitted a simple and immediate identification of the tensor invariants from which the dimensionality and (for 2D structures) the anisotropy of the underlying geoelectric structure could be inferred. Moreover, the variation in dimensionality and anisotropy with depth became immediately apparent when a series of suitably colour-coded, computer-generated Mohr circles covering a whole range of frequencies were displayed on the same diagram.

In two subsequent papers, Lilley (1998a, b) explored various ways of decomposing the MT tensor, and introduced two types of Mohr circles plotted with respect to different axes to illustrate his discussion. The circles were particularly useful for displaying relevant invariants and as visual aids in the theoretical development. They were also plotted over a frequency range of several decades to demonstrate the nature of the BC87 data (Jones et al., 1988), which were analysed in the second paper using the methods proposed in the first.

INVARIANTS OF THE MT TENSOR

Rotational invariants not only define a given tensor in terms of its intrinsic structure, which is independent of the coordinate system chosen, but also are attractive in the MT context because they are not subject to errors associated with a misalignment of the equipment with the usual north and east axes of measurement. Each invariant may also have a distinct physical interpretation that can shed light on the properties of the underlying conductive earth. The tensor invariants, in fact, may be the preferred parameters to use in inversion schemes.

In their analysis of the rotational invariants of the MT tensor, Szarka and Menvielle (1997) proved that there were seven independent invariants. They highlighted two different sets as being particularly useful. The first was a 'classical MT' set comprising the real and imaginary parts of the trace of **M**, the real and imaginary parts of the difference of its off-diagonal elements, and the three invariants associated with the complex determinant of **M**. The second was a 'mathematical' set comprising the final five in the preceding MT set, plus two more associated with the sums of squares of all the elements of **M**. The authors identified their invariants as geometric properties of both the Mohr circles and the Eggers ellipses in the complex plane, but concluded that 'For most real-valued invariants…the complex-plane representation is not very attractive'.

Motivated by Szarka and Menvielle's study, Weaver et al. (2000) devised yet another set of invariants that had a direct physical interpretation. They also plotted both the real and imaginary Mohr circles on the same diagram, which allowed them not only to associate six invariants with obviously independent geometric invariants of the separate Mohr circles, but also to identify the seventh invariant that provides the connecting link between the two circles.

Writing $\mathbf{M} = \mathbf{P} + i\mathbf{Q}$, we obtain by analogy with (3),

$$(P_{11} - \xi_1)^2 + (P_{12} - \xi_4)^2 = \xi_2^2 + \xi_3^2 , \qquad (5)$$

$$(Q_{11} - \eta_1)^2 + (Q_{12} - \eta_4)^2 = \eta_2^2 + \eta_3^2 , \qquad (6)$$

where, following the notation in (1), we have defined

$$\mathbf{P} = \begin{pmatrix} \xi_1 + \xi_3 & \xi_2 + \xi_4 \\ \xi_2 - \xi_4 & \xi_1 - \xi_3 \end{pmatrix}, \quad \mathbf{Q} = \begin{pmatrix} \eta_1 + \eta_3 & \eta_2 + \eta_4 \\ \eta_2 - \eta_4 & \eta_1 - \eta_3 \end{pmatrix}. \qquad (7)$$

Equations (5) and (6) are the Mohr circles shown in Figure 1. The points P_0 and Q_0 represent the actual measured values of the MT tensor components when the x- and y-axes are directed north and east respectively. As the axes are rotated through an angle θ in a right-handed sense about the positive z-axis, the points P and Q rotate anticlockwise around the Mohr circles through an angle 2θ. Clearly, the centres and radii of the circles remain invariant as θ varies, thus immediately yielding ξ_1, ξ_4, η_1, η_4, ξ_0, and η_0 as six

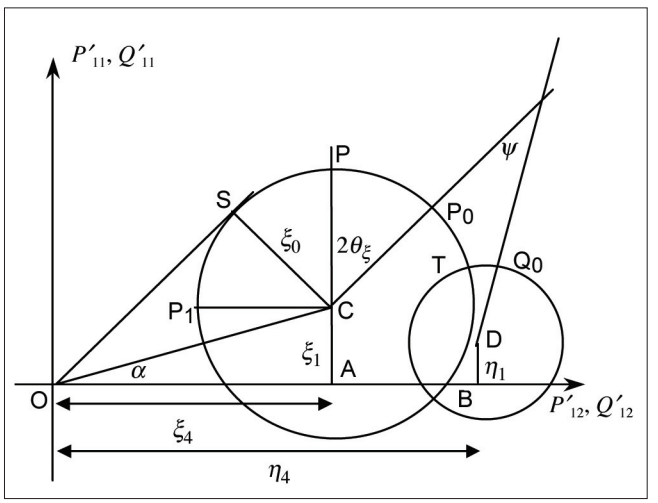

Fig. 1. Real and imaginary Mohr circles for the MT tensor. P rotates anti-clockwise around the Mohr circle through an angle 2θ from the initial point P_0 as the axes of measurement are rotated through an angle θ about the positive z-axis. The diagonal element P'_{11} attains its maximum value when $\theta = \theta_\xi$. The point P_1, corresponding to $\theta = \theta_\xi + \pi/4$, lies on the horizontal axis $P'_{11} = 0$ when $\xi_1 = 0$, and gives the strike angle when the structure is 2D. Similar arguments apply to the point Q and the angle θ_η on the imaginary circle.

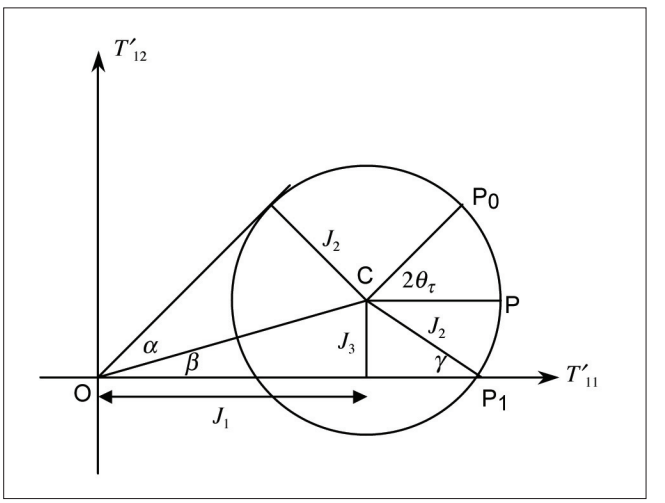

Fig. 2. Mohr circle representation of the phase tensor. Note the different orientation of the axes with T'_{11} the horizontal axis and T'_{12} vertical. Here the point P rotates clockwise around the Mohr circle through an angle 2θ as the axes of measurement rotate through an angle θ about the positive z-axis. θ_τ is the Bahr angle, which gives the strike direction when the regional structure is 2D.

independent invariants. (Here $\xi_0^2 = \xi_2^2 + \xi_3^2$ and $\eta_0^2 = \eta_2^2 + \eta_3^2$ by analogy with the previous definition of τ_0.) The seventh invariant is given by the angle ψ at which the radii to the measured points P_0 and Q_0 intersect. Simple geometry shows that the angle between these radii remains fixed as P and Q rotate around their respective circles. Note that if C and D lie on the horizontal axis, i.e., $\xi_1 = \eta_1 = 0$, then by (2) there will exist an angle $\theta_s = \theta_\xi + \pi/4 = \theta_\eta + \pi/4$ such that the diagonal elements of the tensor $\mathbf{M}$ vanish. Since θ_ξ and θ_η are defined analogously to θ_τ in (2), it follows that $\tan 2\theta_s = -\cot 2\theta_\xi = -\xi_3/\xi_2$ and $\tan 2\theta_s = -\cot 2\theta_\eta = -\eta_3/\eta_2$, whence $\xi_2\eta_3 = \xi_3\eta_2$. This result implies $\psi = 0$ (Weaver et al., 2000), i.e., that CP_0 and DQ_0 in Figure 1 are parallel, an expected result since $\theta_\xi = \theta_\eta$ in this case. These are the necessary conditions for the underlying structure to be 2D with θ_s the angle of strike. If the circles shrink to points on the axis ($\xi_1 = \xi_2 = \xi_3 = \eta_1 = \eta_2 = \eta_3 = 0$) then necessary conditions for a 1D earth are satisfied.

The actual invariants chosen by Weaver et al. (2000) as an aid to the physical interpretation of the data were closely related to, but not identical with the seven listed above. In Figure 1 six of them are represented by the lengths OC and OD, the sines of the angles $\angle$COS and $\angle$DOT (where OS and OT are tangents from the origin to the real and imaginary circles respectively), $\sin(\beta + \alpha)$ and $\sin(\beta - \alpha)$, where $\beta = \angle\mathsf{DOB}$ (not shown). The seventh invariant was related to ψ in a somewhat obscure way, but was chosen such that small absolute values (≤ 0.1) were indicative of weak three-dimensionality in the underlying structure. The numerical values of the other invariants then discriminated between 2D and 1D structures, 2D regional structures with superimposed in-phase galvanic distortion, and other less likely occurrences.

THE PHASE TENSOR

In a recent presentation and paper, Caldwell et al. (2002, 2004) introduced a 'phase tensor', which is defined in the notation of this paper by the 2 × 2 *real* matrix $\mathbf{T} \equiv \mathbf{P}^{-1}\mathbf{Q}$. An important property of this tensor is that it is unaffected by in-phase, galvanic distortion caused by the accumulation of charge on the boundary of a localized, near-surface, conductivity anomaly. To prove this, let $\overline{\mathbf{e}}$ and $\overline{\mathbf{b}}$ denote the *regional* field; the measured field is then $\mathbf{e} = \mathbf{A}\overline{\mathbf{e}}$, $\mathbf{b} = \overline{\mathbf{b}}$, where $\mathbf{A}$ is a *real* matrix representing the distortion. It follows that the *regional* MT tensor $\overline{\mathbf{M}}$ is related to the measured MT tensor $\mathbf{M}$ through the equation $\mathbf{Mb} = \mathbf{e} = \mathbf{A}\overline{\mathbf{e}} = \mathbf{A}\overline{\mathbf{M}}\mathbf{b}$, whence $\mathbf{M} = \mathbf{A}\overline{\mathbf{M}} = \mathbf{A}\overline{\mathbf{P}} + i\mathbf{A}\overline{\mathbf{Q}}$, and

$$\mathbf{T} = \mathbf{P}^{-1}\mathbf{Q} = (\mathbf{A}\overline{\mathbf{P}})^{-1}\mathbf{A}\overline{\mathbf{Q}} = \overline{\mathbf{P}}^{-1}\mathbf{A}^{-1}\mathbf{A}\overline{\mathbf{Q}} = \overline{\mathbf{P}}^{-1}\overline{\mathbf{Q}} = \overline{\mathbf{T}} \ . \qquad (8)$$

Another important property of the phase tensor is its symmetry when the regional conductivity is 2D. For, in the strike frame of a 2D region, rotated through an angle θ_s from the frame of measurement, the diagonal elements of $\overline{\mathbf{P}}'$ and $\overline{\mathbf{Q}}'$ vanish, so that

$$\mathbf{T}' = \overline{\mathbf{T}}' = \left(\overline{\mathbf{P}}'\right)^{-1}\overline{\mathbf{Q}}' = \begin{pmatrix} \overline{Q}'_{21}/\overline{P}'_{21} & 0 \\ 0 & \overline{Q}'_{12}/\overline{P}'_{12} \end{pmatrix} . \qquad (9)$$

Hence by (2), it follows that $\tau_4 = 0$, i.e., $T_{12} = T_{21}$, and that the strike angle is given by $\theta \equiv \theta_s = \theta_\tau$, i.e.,

$$\tan 2\theta_s = \frac{\tau_2}{\tau_3} = \frac{T_{12} + T_{21}}{T_{11} - T_{22}} = \frac{\xi_1\eta_2 - \xi_2\eta_1 - \xi_3\eta_4 + \xi_4\eta_3}{\xi_1\eta_3 - \xi_3\eta_1 + \xi_2\eta_4 - \xi_4\eta_2} \ . \qquad (10)$$

The last term is expressed in terms of the components of the MT tensor itself rather than the phase tensor. It is the well-known formula for the Bahr angle (Bahr, 1988; Weaver et al., 2000) giving the strike angle of a regional 2D structure when localised 3D galvanic distortion is present. If the regional structure is 1D, then the tensors $\overline{\mathbf{P}}'$ and $\overline{\mathbf{Q}}'$ both have equal off-diagonal elements $\overline{P}$ and $\overline{Q}$ in all rotated frames. Thus (9) becomes $\mathbf{T} = \overline{\mathbf{T}} = \mathbf{I}\tan\varphi$ in the frame of measurement, where $\mathbf{I}$ is the identity matrix and $\varphi = \arctan(\overline{Q}/\overline{P})$ is the impedance phase of the 1D regional structure.

Without further information, such as measurements of the vertical magnetic field or prior geological knowledge, it is not known whether the x'-axis or the y'-axis defines the direction of the geoelectric strike in the rotated coordinate system. Both orientations satisfy the conditions of regional two-dimensionality since both $\theta_s = \theta_\tau$ and $\theta_s = \theta_\tau \pm \pi/2$ (along with $\tau_4 = 0$) make $\mathbf{T}'$ diagonal in (2). Thus with no more inherent ambiguity than is already present, the strike angle can be defined as $\theta_s = [\arctan(\tau_2/\tau_3)]/2$, where the principal value of the inverse tangent limits θ_s to the range $-\pi/4 \leq \theta_s \leq \pi/4$. Alternatively, a strike angle defined by $[\arctan(\tau_2/\tau_3)]/2$ for $\tau_2/\tau_3 \geq 0$, and $[\arctan(\tau_2/\tau_3)]/2 + \pi/2$ for $\tau_2/\tau_3 < 0$, will always lie in the first quadrant. In both cases, it is understood that θ_s gives either the direction of the strike itself, or the direction perpendicular to the strike. On the other hand, there is no ambiguity in the definition of θ_τ. The signs of τ_2 and τ_3 determine in which of the four quadrants $2\theta_\tau$ lies, and θ_τ itself is defined in the range $-\pi/2 \leq \theta_\tau \leq \pi/2$.

Caldwell et al. (2004) display the phase tensor as an ellipse in the *xy*-plane using the formulation of Bibby (1986) for the DC apparent resistivity tensor. This is an attractive way of mapping the tensor over the region of interest. Once again, however, the Mohr circle offers an alternative method of representation, which Weaver et al. (2003) found useful in a discussion of the tensor invariants.

In Figure 2, we have plotted the Mohr circle defined by equation (3) with $J_1 = \tau_1$, $J_2 = \tau_0$ and $J_3 = \tau_4$. Here the point P moves around the circle clockwise through an angle 2θ, starting at P_0, as the (x, y)-axes are rotated in a right-handed sense through an angle θ about the z-axis. Weaver et al. (2003) showed how the three invariants J_1, J_2, and J_3 were connected to the MT invariants they had previously introduced, and how similar physical interpretations of the data could be made with them. Thus a 2D regional structure, which implies symmetry of $\mathbf{T}$, requires $\tau_4 = 0$ by virtue of (4), and therefore a vanishing (or in practice small) J_3, with the result that the centre of the circle is located on (or near) the T'_{11}-axis. A 1D structure implies that $\mathbf{T}$ is proportional to $\mathbf{I}$ which, by (4), requires $\tau_0 = \tau_4 = 0$, or $J_2 = J_3 = 0$. In this case the Mohr circle reduces to a point on the T'_{11}-axis. Equation (2) shows that, in general, θ_τ is interpreted as that angle at which T'_{11} attains its extremum value $\tau_1 + \tau_4 = J_1 + J_3$ on the Mohr circle, as depicted by the position of point P in Figure 2. If the regional structure is 2D, then P and P_1, the point where the circle intersects the T'_{11}-axis, are coincident and $\theta_\tau = \theta_s$. Otherwise, the magnitude of the angle $\gamma = \arcsin(J_3/J_2)$ is a measure of the offset of the centre of the circle from the axis, and therefore of the departure from regional two-dimensionality. It can also be regarded as an estimate of the uncertainty in $2\theta_s$. In fact, as emphasised by Weaver et al. (2003), the ratio $|J_3/J_2|$ is *precisely* the magnitude of the seventh invariant (related to ψ) of Weaver et al. (2000), even though it was based on quite different reasoning.

A simple decomposition of $\mathbf{T}$ expressed in the form (4) is

$$\mathbf{T} = J_1\mathbf{I} + J_2\mathbf{J} + J_3\mathbf{K} \ , \qquad (11)$$

where $\mathbf{J} = \mathbf{K}_1\cos 2\theta_\tau + \mathbf{K}_2\sin 2\theta_\tau$, and

$$\mathbf{K}_1 = \begin{pmatrix} 1 & 0 \\ 0 & -1 \end{pmatrix} \quad \mathbf{K}_2 = \begin{pmatrix} 0 & 1 \\ 1 & 0 \end{pmatrix} \quad \mathbf{K} = \begin{pmatrix} 0 & 1 \\ -1 & 0 \end{pmatrix} . \qquad (12)$$

With a strictly 1D regional structure, $J_2 = J_3 = 0$ and only the first term of (11) contributes to the phase tensor. In a 2D case, $J_3 = 0$ and the first two terms contribute. A fully 3D regional structure implies that all three terms in (11) are significant. Thus the first, second, and third terms in (11) can be regarded as the 1D, 2D, and 3D contributions to the phase tensor respectively. In practice, if $(J_2^2 + J_3^2)^{1/2} << |J_1|$ (or $|\sin\alpha| << 1$ and $|\sin\beta| << 1$ in Figure 2) we may assert that the data are consistent with a 1D regional structure; otherwise, if $|J_3| << |J_2|$ (or $|\sin\gamma| << 1$) they are consistent with a 2D regional structure. In both cases, it is immaterial whether the data have been subjected to local 3D galvanic distortion.

CONCLUSIONS

The original idea of adapting the Mohr circle representation of the real, symmetric stress tensor in elasticity theory to the complex, generally asymmetric MT tensor in geo-electromagnetism has been shown to be useful as a graphical aid in interpreting MT data. In particular, the rotational invariants of the MT tensor, which have their own physical interpretations, are readily identifiable on a Mohr circle diagram, while the radii and off-axis displacements of the circles indicate the dimensionality of the underlying geoelectric structure. In this regard, plots of Mohr circles over a range of periods give a strong visual impression of the type of data under analysis.

A major drawback in representing a complex tensor is that two Mohr circles are required, one to represent the real part of the tensor and the other the imaginary part. In this paper, we have exploited the newly defined 'phase tensor' of Caldwell et al. (2004), which encapsulates many of the important properties of MT data. Since the phase tensor is real, it can be ideally represented by a single Mohr circle with only three rather than seven rotational invariants. The three salient physical invariants, which are associated with 1D, 2D, and 3D regional structures, are immediately identifiable as the three obvious geometric invariants of the circle, the coordinates of its centre and its radius. Moreover, the angle of strike in 2D (or near 2D) cases is also visible on the diagram, as is the 'uncertainty angle', representing the strength of 3D effects and therefore the relevance of the concept of strike angle. It is hoped that the single Mohr circle representing the phase tensor will become an even more useful aid in the visualisation and treatment of MT data than the real and imaginary circles representing the complex MT tensor itself.

ACKNOWLEDGEMENTS

The authors thank the two referees for their helpful suggestions and comments, all of which have been taken into account while preparing the final version of this paper. This collaborative work began in 1996 when JTW was a Visiting Fellow at the Research School of Earth Sciences in the Australian National University, and continued during a subsequent visit in 2003. JTW thanks Ted Lilley for his warm and generous hospitality and ANU for its support during the two visits.

REFERENCES

Bahr, K., 1988, Interpretation of the magnetotelluric impedance tensor: regional induction and local telluric distortion: *Journal of Geophysics*, **62**, 119–127.

Bibby, H.M., 1986, Analysis of multiple-source bipole- quadrupole resistivity surveys using the apparent resistivity tensor: *Geophysics*, **51**, 972–983.

Caldwell, T.G., Bibby, H.M., and Brown, C., 2002, The magnetotelluric phase tensor—a method of distortional analysis for 3D regional conductivity structures: *16th Workshop on Electromagnetic Induction in the Earth, Santa Fe, New Mexico, USA*, Abstract EM12–4.

Caldwell, T.G., Bibby, H.M., and Brown, C., 2004, The magnetotelluric phase tensor: *Geophysical Journal International*, **158**, 457–469.

Eggers, D.E., 1982, An eigenstate formulation of the magnetotelluric impedance tensor: *Geophysics*, **47**, 1204–1214.

Jones, A.G., Kurtz, R.D., Oldenburg, D.W., Boerner, D.E., and Ellis, R., 1988, Magnetotelluric observations along the LITHOPROBE southeastern Canadian cordilleran transect: *Geophysical Research Letters*, **15**, 677–680.

Lilley, F.E.M., 1976, Diagrams for magnetotelluric data: *Geophysics*, **41**, 766–779.

Lilley, F.E.M., 1993a, Mohr circles in magnetotelluric interpretation (i) simple static shift; (ii) Bahr's analysis: *Journal of Geomagnetism and Geoelectricity*, **45**, 833–839.

Lilley, F.E.M., 1993b, Three-dimensionality of the BC87 magnetotelluric data set studied using Mohr circles: *Journal of Geomagnetism and Geoelectricity*, **45**, 1107–1113.

Lilley, F.E.M., 1993c, Magnetotelluric analysis using Mohr circles: *Geophysics*, **58**, 1498–1506.

Lilley, F.E.M., 1998a, Magnetotelluric tensor decomposition: Part I, Theory for a basic procedure: *Geophysics*, **63**, 1885–1897.

Lilley, F.E.M., 1998b, Magnetotelluric tensor decomposition: Part II, Examples of a basic procedure: *Geophysics*, **63**, 1898–1907.

Szarka, L., and Menvielle, M., 1997, Analysis of rotational invariants of the magnetotelluric impedance tensor: *Geophysical Journal International*, **129**, 133–142.

Weaver, J.T., Agarwal, A.K., and Lilley, F.E.M., 2000, Characterization of the magnetotelluric tensor in terms of its invariants: *Geophysical Journal International*, **141**, 321–336.

Weaver, J.T., Agarwal, A.K., and Lilley, F.E.M., 2003, The relationship between the magnetotelluric invariants and the phase tensor of Caldwell, Bibby and Brown: in Macnae, J., and Liu, G. (eds.), "*Three-Dimensional Electromagnetics III*", Australian Society of Exploration Geophysicists, paper 43, 1–8.